Figures-of-Merit and current metric for the comparison of IGCTs and IGBTs in Modular Multilevel Converters

Arthur Boutry, Cyril Buttay, Dong Dong, Rolando Burgos, Bruno Lefebvre, Florent Morel, Colin Davidson

▶ **To cite this version:**

Arthur Boutry, Cyril Buttay, Dong Dong, Rolando Burgos, Bruno Lefebvre, et al.. Figures-of-Merit and current metric for the comparison of IGCTs and IGBTs in Modular Multilevel Converters. 2020 CPES Annual conference, Center for Power Electronic Systems, Aug 2020, Blacksburg, VA, United States. hal-04525165

HAL Id: hal-04525165
https://hal.science/hal-04525165

Submitted on 28 Mar 2024

HAL is a multi-disciplinary open access archive for the deposit and dissemination of scientific research documents, whether they are published or not. The documents may come from teaching and research institutions in France or abroad, or from public or private research centers.

L'archive ouverte pluridisciplinaire **HAL**, est destinée au dépôt et à la diffusion de documents scientifiques de niveau recherche, publiés ou non, émanant des établissements d'enseignement et de recherche français ou étrangers, des laboratoires publics ou privés.

Distributed under a Creative Commons Attribution 4.0 International License

Figures-of-Merit and current metric for the comparison of IGCTs and IGBTs in Modular Multilevel Converters

Arthur Boutry[†‡], Cyril Buttay[‡], Dong Dong[*], Rolando Burgos[*], Bruno Lefebvre[†], Florent Morel[†], and Colin Davidson[§]

[*]Center for Power Electronics Systems
The Bradley Department of Electrical and Computer Engineering
Virginia Polytechnic Institute and State University Blacksburg,
VA 24061 USA
[†]SuperGrid Institute,
69628 Villeurbanne, France
[‡] Univ Lyon, INSA Lyon, Ampère UMR CNRS 5005,
Laboratoire Ampère
69621 Villeurbanne, France
[§]GE Grid Solutions
Stafford, United Kingdom

***Abstract*—IGCTs and IGBTs are compared in the case of a HVDC MMC. Specific figures of merit, and a current metric providing simple means to compare them, are introduced and discussed. Simulation results of a MMC model and figures of merit are shown to provide consistent result, proving that the proposed figures of merit are a very simple and fast way to select the best semiconductor switch. Furthermore, our analysis supports the growing interest in IGCTs for MMCs, as they are found to produce the lowest level of losses.**

I. Introduction

The Modular Multilevel Converter (MMC) is a Voltage Source Converter (VSC) developed and used for Medium or High Voltage Direct Current (MVDC or HVDC) applications. This is a reversible, AC/DC Converter. The MMC (fig. 2) is based on submodules (SMs), its elementary building blocks. Mainly composed of switches and a capacitor, a submodule can be seen as a small voltage source that can be inserted or not (depending on the switching sequence and the current sign along the submodules). The main type of submodule has a half-bridge topology, consisting in two switches and their freewheeling diode, one capacitor and auxiliary systems.

Most submodule designs rely on IGBTs as the semiconductor switch. This is the case, for example in HVDC-MMCs produced by General Electric, ABB, Siemens [1] or RXPE [2]. Indeed, IGBT modules offer high voltage ratings up to $6.5\,\mathrm{kV}$, high current ratings, are fully controllable with little power, and can be sourced from many suppliers. On the contrary, thyristors, which are often used in other HVDC converters would require a complex circuitry to be turned-off. In theory, high voltage SiC MOSFETs would be ideal components for such application, but their cost is currently prohibitive.

Several authors [3]–[5] have investigated the possibility of using IGCTs (a type of gate-controlled thyristor that can be turned off without parallel-type snubber) in a MMC. They demonstrated that doing so would increase the conversion efficiency of a MMC as compared to using IGBTs. Note that IGCTs require a series-type snubber to limit the switching speed and protect the associated freewheeling diode when the IGCT turns on [6], [7]. Even considering the additional power dissipation caused by this snubber circuit, IGCTs were found more efficient than IGBTs in the case of an MMC.

However, because of the very different principles IGBTs and IGCTs operate on, they cannot be compared directly from the figures quoted in their datasheets. Therefore, there is a concern that the advantage if IGCTs over IGBT could result from a biased comparison, using devices with very different ratings. In this paper, we introduce new Figures Of Merit (FOMs), as a means for easy and accurate selection of semiconductor switches for an MMC application.

The validity of these FOMs is then assessed against a dynamic MMC model: unlike an average model, the waveforms, the on-state voltages and the losses are calculated at each instant such model provides realistic waveforms, realistic losses. In particular, the actual switching frequency and switching instants of the semiconductor devices is an outcome of the simulation (MMCs do not operate at a constant frequency) and not a parameter.

II. Comparison between IGCTs and IGBTs

A. General considerations and features

The table I provides a general comparison of IGCTs and IGBTs.

The IGCT is the result of the evolution of the thyristor technology. The simplest type of thyristor is the SCR (Silicon

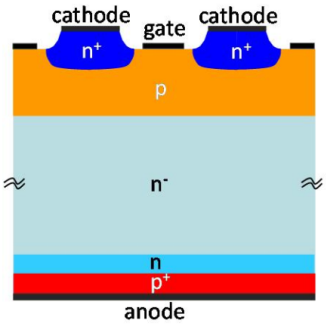

(a) Internal structure of a GCT [10]

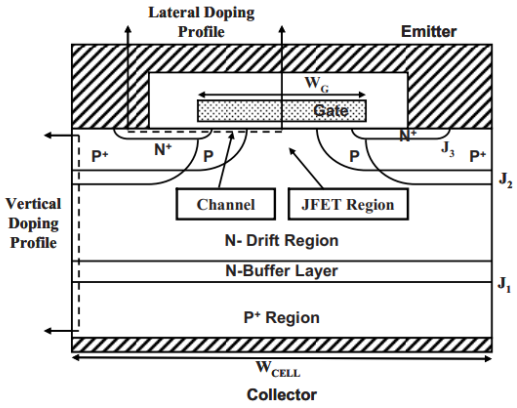

(b) Structure of an asymetric IGBT [11]

Fig. 1: IGCTs and IGBTs structures

Controlled Rectifier). It is a semiconductor device made of four layers (P+N-PN+ structure) turned-on by a current pulse. The GTO (Gate Turn-Off) thyristor was introduced in 1980 [8]. Compared to the SCR, it offers a controlled turn-off capability by applying a negative voltage to the gate. The GCT is an evolution of the GTO. Two improvements are the base of the GCT: a low-inductive housing-design allowing a quick, more homogeneous turn-off without filamentation, and a "transparent emitter buffer layer". The buffer-layer and transparent emitter technologies consist in a weakly doped n-layer located between the n-base and the p-emitter. This results in reductions in on-state voltage and turn-off energies. The low-inductive structure of the GCT allows to rapidly redirect all the anode current from the cathode to the gate at turn-off. This prevents filamentation [9] and reduces turn-off times (10 µs for GCTs compared to 100 µs for GTOs). Another consequence is a much better immunity to dV/dt, removing the need for a turn-off snubber. The asymmetric device cross-section and its top view can be found in figure 1a. The IGCT (Integrated GCT) corresponds to a GCT switch attached with its gate drive circuit.

The IGBT is a voltage-driven semiconductor developed in the early 1980s using a combination of a MOSFET and a N-P-N transistor structure. [11] This structure can be seen on

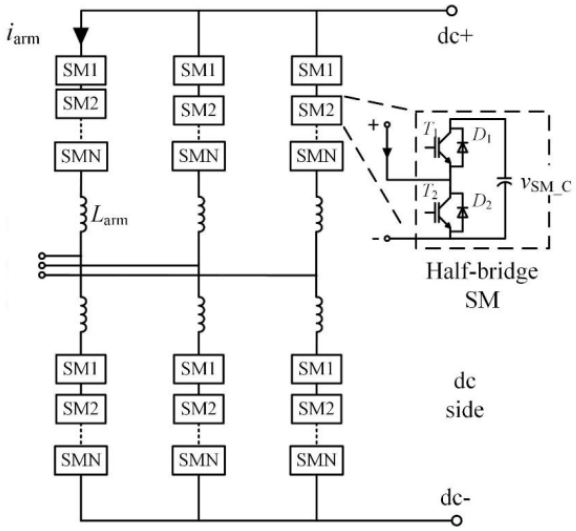

Fig. 2: Circuit Diagram of the modular multilevel converter [17] and of one of its submodules (SM)

figure 1b. Its relatively low losses and its ability operate at high frequencies (several kilohertz) make it widely used in many fields. It requires a simple gate unit with a low power consumption. Compared to the GCT or other thyristors, which are made on a single semiconductor wafer, IGBT modules are formed by paralleling a number of smaller semiconductor chips, making it scalable to different power ratings.

The technologies are still being improved with new structures for the IGBT (Enhanced Trench IGBTs – TSPT+ – for ABB [12], or the Injection Enhancement Gate Transistor – IEGT – for Toshiba [13]) and the IGCT (Reverse Conducting IGCT, Reverse Blocking IGCT... [10]), pushing their limits with higher ratings [10], [12], [14], [15], lower on-state voltage and switching losses [10], [16].

B. Current ratings of semiconductor switches

Many values are quoted in the datasheet of a semiconductor switch regarding the on-state current they can manage. These current values and those introduced in this paper are described in table II. For the IGCT, none of them can be directly and simply linked to the MMC operation, unlike for the IGBT (for which the DC-current rating on the IGBT datasheet corresponds to the maximum current going through the IGBT in MMC operation). As a consequence, the suitability of an IGCT for a given MMC cannot be assessed directly, and no direct comparison can be done between IGBTs and IGCTs.

Thus, a new current metric ($I_{eq-IGCT}$) has to be defined to compare efficiently IGCTs and IGBTs current capabilities. This new current metric should correspond to a generic MMC case (it is not specific to one MMC implementation in particular) and has of course to be based on data available in the IGCT datasheet. The goal is to build a current metric

TABLE I
GLOBAL COMPARISON OF IGCTS AND IGBTS (PRESS-PACK)

Semiconductor	**IGCT**	**IGBT (Press-Pack)**
Snubber	Needed (series, to limit turn-on dI/dt)	No
On-state Voltage	Low (around 2V at high current)	High (more than 3V at high current)
Turn-on Energy loss	Around 2 J (2.8 kV, 2 kA)	Around 10 J (2.8 kV, 2 kA)
Turn-off Energy loss	Around 10 J (2.8 kV, 2 kA)	Around 10 J (2.8 kV, 2 kA)
Gate circuit	Large, and high power consumption [18]	Small, low power consumption [18]
Switching Frequency	Low (up to 350 Hz) [10]	High (up to tens of kHz) [19]

TABLE II
DESCRIPTIONS OF THE CURRENT-RELATED VARIABLES MENTIONED IN THE PAPER.

Current	**Switch**	**Source**	**Description**	**Symbol**
DC-current	IGBT	Datasheet	Max. DC-current that the IGBT can conduct	$I_{dc-igbt}$
Peak Current	IGBT	Datasheet	Max. peak (1ms) current that the IGBT can switch	$I_{pk-igbt}$
Max. average on-state current	IGCT	Datasheet	Based on half-sine, no real practical meaning according to [20]	$I_{av-igct}$
Max. RMS on-state current	IGCT	Datasheet	Based on half-sine, no real practical meaning according to [20]	$I_{rms-igct}$
Max. controllable turn-off current	IGCT	Datasheet	Max. anode current that can be turned-off	$I_{mto-igct}$
Switching Current	Both	Datasheet	Condition test current for the switching energy in the datasheet	I_{swi}
Max. av. current MMC	Both	This paper	Av. current going through the switches (worst case)	$I_{av-semi}$
Max. instantaneous current MMC	Both	This paper	Max. instantaneous current seen by the switches	$I_{max-semi}$
Equivalent current IGCT	IGCT	This paper	Built with the datasheet currents, equivalent of $I_{dc-igbt}$ for the IGCT	$I_{eq-igct}$

comparable to the DC-current quoted in IGBT datasheets $I_{dc-igbt}$, considering the actual current waveforms in a MMC.

The worst case for the IGCT – i.e. when the IGCT is subject to the maximum possible current – is when the submodule is inserted for an entire period. Considering the asymmetric operation of the MMC, one of the IGCT will be subject to more current than the other. This IGCTs currents have their waveforms drawn in figure 3, assuming the current of the AC output of the MMC is perfectly sinusoidal. It can be seen that this waveform is close to a 50 Hz half-sine. The adopted approach is to calculate the average current of that waveform in the general case and link to the maximum current value of the same waveform. By establishing this connection between $I_{av-semi}$ and $I_{max-semi}$, and based on $I_{av-IGCT}$ we can introduce $I_{eq-igct}$, which is the equivalent for the IGCT of the dc current for an IGBT ($I_{dc-igbt}$, quoted in the device datasheet). The waveforms of the MMC are described in eqs. (1a) and (1b), with i_a, the current on the AC-side, I_{arm} the current through the considered arm and I_d the current on the DC-side. Here, it will be considered that the arm is the one described in equation 1b, but the same reasoning can be used with any arm and any power factor.

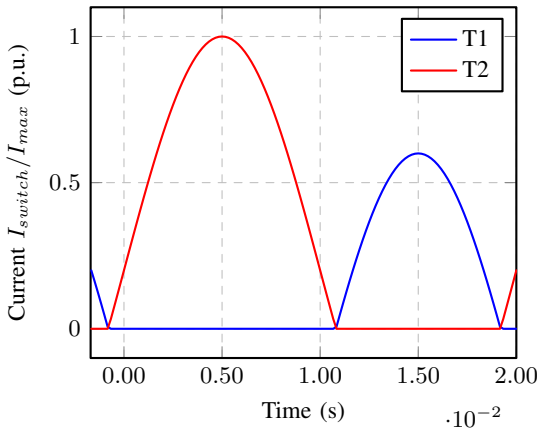

Fig. 3: Currents in the power switches, if the submodule is kept inserted (worst case).

$$i_a = I_a * sin(\omega t) \tag{1a}$$

$$I_{arm}(t) = \frac{I_d}{3} + \frac{I_a}{2}\sin\omega t \tag{1b}$$

A MMC can be described with the following design-related ratios (eqs. (2a) and (2b)), k being the ratio between the AC and DC currents, and m being the ratio between the ratio between the AC and DC voltages. The relation between those ratios and the power factor is the eq. (2c), resulting from the hypothesis that the powers from each side (AC and DC) are equal. Typical values for m is around 0.8 ± 0.1 and for $\cos(\phi)$ is around 0.85 ± 0.1 too. So the typical value of k is around 3 ± 1.

$$k = \frac{3I_a}{2I_d} \tag{2a}$$

$$m = \frac{2U_a}{U_d} \tag{2b}$$

$$k * m * \cos(\phi) = 2 \tag{2c}$$

The calculation of the average current through the IGCT is described in eqs. (3a) to (3d), with the integration of the

positive component of the arm current, corresponding to the current in the most loaded IGCT. The arm current is positive between t_1 and t_2, described in (3a). The average current of the IGCT is obtained in eq. (3d).

$$t_1 = \frac{\arcsin\left(-\frac{1}{k}\right)}{\omega}; t_2 = \frac{\pi - \arcsin\left(-\frac{1}{k}\right)}{\omega} \tag{3a}$$

$$I_{av-semi} = \frac{1}{T}\int_{t_1}^{t_2} I_{arm}(t)dt = \frac{1}{T}\int_{t_1}^{t_2}[\frac{I_d}{3} + \frac{I_a}{2}\sin\omega t]dt \tag{3b}$$

$$I_a = \frac{2k}{3}I_d \tag{3c}$$

$$I_{av-semi} = \frac{I_d}{3T} * (t_2 - t_1) + \frac{kI_d}{6\pi}[-\cos(\omega t_2) + \cos(\omega t_1)] \tag{3d}$$

This expression of $I_{av-semi}$ can be simplified using a linear regression, shown in eq. (4a). This regression is done on a limited range of values of k, between 2, minimum of k in half-bridge based MMCs according to according eq. 2c and 10, corresponding to normal half-bridge based MMCs, 10 being chosen high for a HVDC MMC. The regression gives a R^2 value of 0.99992.

$$I_{av-semi} = I_d * [\alpha * k + \beta] \tag{4a}$$

$$\alpha = 0.103398; \beta = 0.19019 \tag{4b}$$

$I_{max-semi}$ is obtained from equation (1b) and equation (2a) by replacing the sinus by maximal value. The function f is then introduced in equation 5b, as the ratio between $I_{max-semi}$ and $I_{av-semi}$.

$$I_{max-semi} = I_d * (\frac{1+k}{3}) \tag{5a}$$

$$f(k) = \frac{I_{max-semi}}{I_{av-semi}} = \frac{1+k}{3 \times (\alpha \times k + \beta)} \tag{5b}$$

An equivalent current $I_{eq-IGCT}$, that can be directly compared to the $I_{dc-igbt}$ of an IGBT, is defined in equation 6. $I_{eq-IGCT}$ is equal to the minimum of $I_{mto-IGCT}$ (maximum current at turn-off) and $I_{av-IGCT} \times f(k)$ to ensure it does not exceed the current that can safely be interrupted.

$$I_{eq-IGCT} = \min(I_{mto-IGCT}, I_{av-IGCT} \times f(k)) \tag{6}$$

f is a function that is increasing with k. Here, we consider the case in which $k = 2$, i.e. $f(k) = 2.5116$, to stay in the most general case. In this case, for many IGCTs, $I_{av-IGCT} \times f(k)$ has a higher value than $I_{mto-igct}$. Two things can be concluded from that result. First, $I_{mto-igct}$ can be most of the times compared to $I_{dc-igbt}$ (even though it needs to be checked afterwards with this method). Then, most available IGCTs have very high $I_{mto-igct}$ (3 to 8 kA), which means they can handle much larger currents than available IGBTs ($I_{dc-igbt} = 1$ to 3 kA for >3.3 kV IGBTs) in a MMC

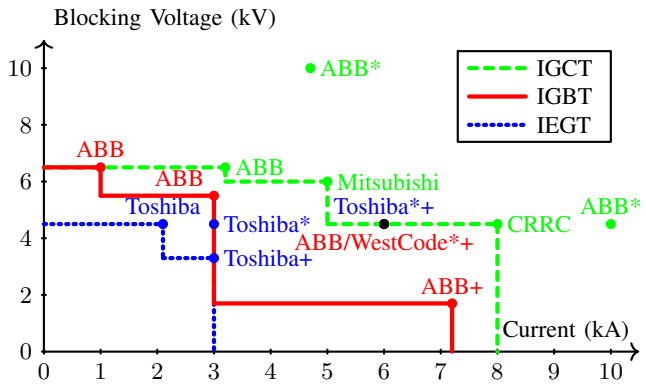

Fig. 4: Ratings of semiconductors (IGBTs, IEGTs and IGCTs), with the blocking voltage and the current calculated in the paper: $I_{dc-igbt}$ for IEGTs and IGBTs and $I_{eq-igct}$ for the IGCTs. '+' means 'not found in catalog but in literature', '*' means 'prototype'. Sources: ABB, Mitsubishi, CRRC, Dynex, Toshiba online catalogs (2019) and [18], [21], [22].

application. This is illustrated in Fig. 4 where $I_{dc-igbt}$ and $I_{eq-IGCT}$ are ploted. Finally, the $I_{mto-igct}$ is a limit of the IGCT related to the gate circuit (how much current the gate can divert to open the IGCT) and $I_{av-IGCT} \times f(k)$ is a thermal related limit of the semiconductor. If $I_{eq-IGCT}$ is equal to $I_{mto-igct}$, the limit is not related to the semiconductor itself: the semiconductor could withstand more current.

C. Figures of merit for conduction and switching losses

After we established a consistent current rating for IGBT and IGCTs in the previous section, we can now use it to compare the merits of different switches. These Figures of Merit (FOMs) are related to the conduction and switching losses.

For the conduction losses, a FOM that can be used is the on-state voltage. As this on-state voltage is dependent on the current flowing through the component, we consider the MMC waveforms to calculate an average on-state voltage value. It is equal to the on-state voltage for the average current, as it is demonstrated in eqs (7a) to (7b).

$$V_{on}(I) = V_0 + R.I \tag{7a}$$

$$average(V_{on}) = V_0 + R.average(I) = V_{on}(I_{av-semi}) \tag{7b}$$

The average on-state voltage is then normalized with respect to the blocking voltage of the switch (considered with a de-rating to reach a reliability of 100 Failure-In-Time – FIT – defined in particular in [23]), to allow the comparison between semiconductors with different voltage ratings. The final figure of merit is then:

TABLE III
LOSS STUDIES RESULTS

	Total losses IGBT (%)	Total losses IGCT (%)	Inverter or rectifier	Loss red. (%)
[5]	0.48	0.41	Average rectifier and inverter	14.6
[3]	0.64	0.44	Rectifier	31
[3]	0.32	0.27	Inverter	15.6
[4]	0.76	0.74	Rectifier	2.6
[4]	0.83	0.64	Inverter	22.9

$$FM_{cond-loss}(IGCT) = \frac{V_{on}(I_{av-igct})}{V_{block-100FIT}} \tag{8a}$$

$$FM_{cond-loss}(IGBT) = \frac{V_{on}(\frac{I_{dc-igbt}}{2.5116})}{V_{block-100FIT}} \tag{8b}$$

For the switching losses, turn-on and turn-off energies are used to compare semiconductors. In datasheets, the losses figures are always quoted at maximum rated current, which may differ from the actual current in the application. The IGBT and IGCT switching losses can be approximated by a linear function depending on the current. For the IGBT this is only true up to the dc-current rating, but this is sufficient in the case of the MMC. To compare the switching losses, the chosen figure of merit is the following:

$$FM_{swi-loss} = \frac{E_{datasheet}}{V_{block-100FIT} \times I_{swi}} \tag{9}$$

III. FOM VALIDATION, SIMULATION AND LOSS STUDY

A. Model Description

As it can be seen in the literature (see Tab. III), IGCTs are always found to cause less losses than IGBTs. However, the estimated amount actually varies noticeably from one publication to another because it depends on many factors: MMC ratings, control methods, operating points, not all of which are disclosed in the corresponding publications. As a consequence, it is difficult to use published results to validate our FOMs. That is why a simple MMC model has been developed, focusing on the individual behavior of each submodule (capacitor and semiconductors). This model is used to validate the validity of the FOM approach.

The model is written as a Matlab script. The modeling assumptions are as follows: perfect sinusoidal current in the arm; arm inductor, line resistors and energy exchange between arms not modeled; only one arm considered.

The model calculates the switching instants of the semiconductors switches with the nearest level modulation control method [24] and the reduced switching algorithm for capacitor voltage balancing [25]. Although simple, this model produces realistic waveforms for the operating voltage and current of each submodule, which allows for a more accurate estimation of the losses than average models. Examples of current and voltage waveforms for the upper arm, and the capacitor voltages for some (randomly chosen) submodules are displayed in figure 5.

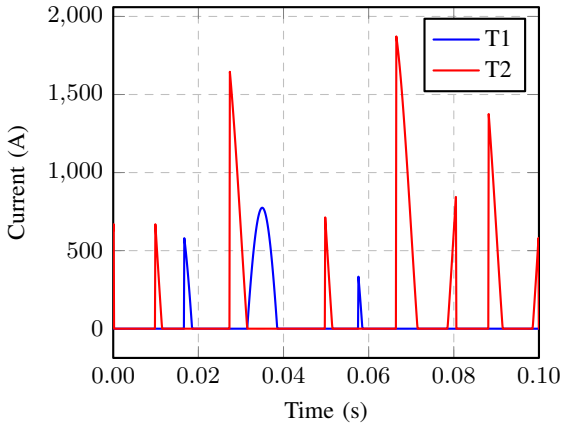

(a) Currents in the semiconductor switches for the SM n°72

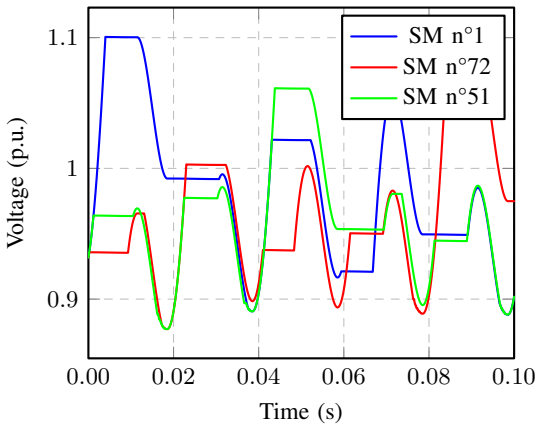

(b) Capacitor Voltages

Fig. 5: Waveforms of the arm and some submodules, after simulation of the same MMC as [4]. (p.u. means per unit and is the instantaneous voltage of the submodule divided by the rated voltage of the submodule)

The waveforms in figure 5b show that, as it is the case in actual MMCs, the different submodules have different switching moments, different voltages at a given time, and they respect the set voltage ripple (10% in that case) around the average value of the capacitors voltages. The waveforms on the figure 5a show that the semiconductor conduction losses are calculated with realistic current waveforms. Those features of the model permit to have more realistic losses figures compared to an average model.

This model has been tested for different durations and the duration of 5 periods is sufficient.

B. Loss Study

A simulation was realized considering the following MMC: 1 GVA, 400 submodules per arm, a mean submodule voltage of 1600 V, a DC voltage of 640 kV (pole to pole). The considered devices are: IGCTs (5SHY 35L4521) and asso-

ciated diodes (5SDF 20L4520), or press-pack IGBTs (5SNA 2000K450300) which include their own diodes. Using the model, losses of 5.2 MW (0.52% of the transferred power) in the case of the IGCT and 6.72 MW (0.672%) in the case of the IGBT have been calculated. This corresponds to a loss reduction of 23.6%, which is consistent with the results presented previously.

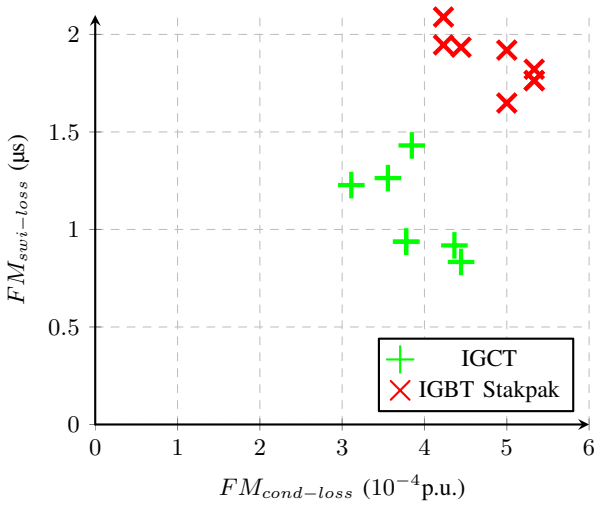

(a) Figures of merit applied to ABB online catalog for IGCTs and Stakpak IGBTs (2019).

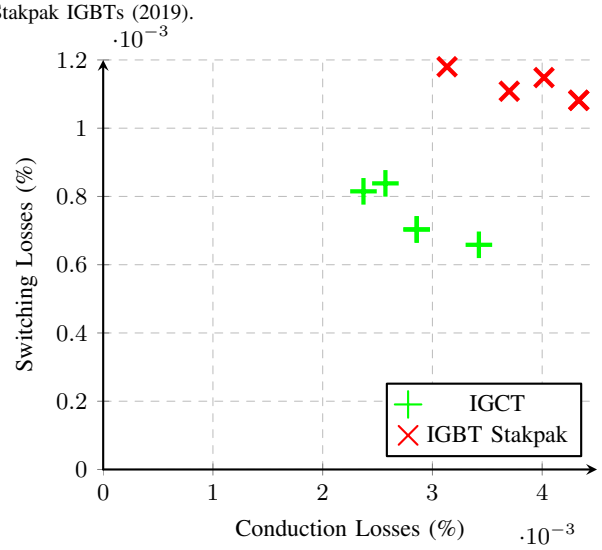

(b) Switching and conduction losses from 4.5 kV ABB IGCTs and Stakpak IGBTs, simulated for the same MMC as [4] (inverter case).

Fig. 6: Figures of merit analysis: displayed and compared to the simulated conduction and switching losses.

C. Analysis of the figures of merit

The figures of merit for the ABB IGCTs and Stakpak IGBTs are displayed on Fig. 6a. They are in good agreement with the corresponding switching and conduction losses calculated using the MMC model (for 4.5 kV devices only, Fig. 6b). Both approaches confirm the superiority of IGCTs

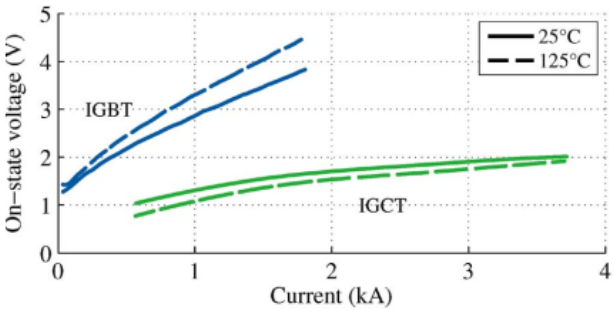

Fig. 7: On-state voltage of one IGCT and one IGBT [18]

over IGBTs regarding losses in general. This demonstrates the interest of those figures of merit: they provide a quick and efficient comparison without the modeling and the simulation of a MMC.

As expected the IGCT has lower conduction losses on average, but in some cases, with the worst IGCT and the best IGBT in terms of conduction losses, the IGBT is better. This appears both in the figure of merit and the simulated conduction losses (see figure 6). It can be explained by the use of average on-state voltage in the figure of merit – calculated as the on-state voltage at the average current of each semiconductor – and by the use of the same MMC for the simulations – the current of this MMC is the same for all the semiconductors. This implies an under-utilization of the IGCTs, whose on-state voltage grows slowly with the current. Indeed, as it can be seen in figure 7, the on-state voltage of an IGCT grows slower than the on-state voltage of an IGBT. In fact, the IGCT is more suitable for MMCs with higher current ratings. But it has to be kept in mind that the figure 7 is a particular case of one IGCT and one IGBT.

Furthermore, the IGCT is often described as having more switching losses than the IGBT: with the figures of merit (and confirmed by the simulation), it can be seen that in any studied case, the IGCT has lower switching losses. This is due to the fact that the turn-on losses are very small for the IGCT.

But it has to mentioned that on figure 6b, the scale is different (0.02% per division for the switching losses and 0.1% per division for the conduction losses). The biggest conduction losses difference (the best IGCT and the worst IGBT in terms of conduction losses) is 0.2% while the biggest switching losses difference is 0.055%. This is due to the low switching frequency of the devices in the case of HVDC MMCs.

IV. Conclusion

In this paper, new metrics have been developed to compare efficiently and quickly IGCTs and IGBTs in the particular case of HVDC MMCs. A current rating and losses figures of merit have been built.

The current rating has shown that the available IGCTs have higher usable current ratings than the available IGBTs. The proposed FOMs offer a simple, analytical way to compare given IGBTs and IGCTs for a HVDC MMC application, and to easily select the best device.

The different simulations have validated the FOMs and confirmed their necessity. Indeed, not all IGCTs are superior (in terms of losses) than IGBTs, and the selection must be performed on a device-per-device basis.

But the FOMs confirm an advantage – in general – of IGCTs over IGBTs regarding converter efficiency, and are consistent with more complex converter-level simulations.

REFERENCES

[1] K. Sharifabadi, L. Harnefors, H.-P. Nee, S. Norrga, and R. Teodorescu, *Design, Control, and Application of Modular Multilevel Converters for HVDC Transmission Systems*. John Wiley & Sons Inc, 2016.

[2] H. Chen, W. Cao, P. Bordignon, R. Yi, H. Zhang, and W. Shi, "Design and testing of the world's first single-level press-pack IGBT based submodule for MMC VSC HVDC applications," in *2015 IEEE Energy Conversion Congress and Exposition (ECCE)*, IEEE, sep 2015.

[3] D. Guédon, P. Ladoux, M. Kanoun, and S. Sanchez, "IGCTs in HVDC systems: Analysis and assessment of losses," in *PCIM Europe 2019*, 2019.

[4] B. Zhao, R. Zeng, J. Li, T. Wei, Z. Chen, Q. Song, and Z. Yu, "Practical analytical model and comprehensive comparison of power loss performance for various MMCs based on IGCT in HVDC application," *IEEE Journal of Emerging and Selected Topics in Power Electronics*, vol. 7, pp. 1071–1083, jun 2019.

[5] T. Modeer, H.-P. Nee, and S. Norrga, "Loss comparison of different submodule implementations for modular multilevel converters in HVDC applications," *EPE Journal*, vol. 22, pp. 32–38, sep 2012.

[6] T. Wei, Q. Song, J. Li, B. Zhao, Z. Chen, and R. Zeng, "Experimental evaluation of IGCT converters with reduced di/dt limiting inductance," in *2018 IEEE Applied Power Electronics Conference and Exposition (APEC)*, IEEE, mar 2018.

[7] R. Zeng, B. Zhao, T. Wei, C. Xu, Z. Chen, J. Liu, W. Zhou, Q. Song, and Z. Yu, "Integrated gate commutated thyristor-based modular multilevel converters: A promising solution for high-voltage dc applications," *IEEE Industrial Electronics Magazine*, vol. 13, pp. 4–16, jun 2019.

[8] J. Lutz, H. Schlangenotto, U. Scheuermann, and R. D. Doncker, *Semiconductor Power Devices*. Springer Berlin Heidelberg, 2011.

[9] S. Alvarez-Hidalgo, *Characterisation of 3.3kV IGCTs for Medium Power Applications*. PhD thesis, ENSEEIHT, 2005.

[10] U. Vemulapati, M. Rahimo, M. Arnold, T. Wikstrom, J. Vobecky, B. Backlund, and T. Stiasny, "Recent advancements in IGCT technologies for high power electronics applications," in *2015 17th European Conference on Power Electronics and Applications (EPE'15 ECCE-Europe)*, IEEE, sep 2015.

[11] B. J. Baliga, *Fundamentals of Power Semiconductor Devices*. Springer, 2008.

[12] C. Corvasce, M. Andenna, S. Matthias, L. Storasta, A. Kopta, M. Rahimo, L. De-Michielis, S. Geissmann, and R. Schnell, "3300v hipak2 modules with enhanced trench (tspt+) igbts and field charge extraction diodes rated up to 1800a," in *PCIM Europe 2016; International Exhibition and Conference for Power Electronics, Intelligent Motion, Renewable Energy and Energy Management*, pp. 1–8, May 2016.

[13] Toshiba, "High-power electric solutions - system catalog," tech. rep., Toshiba, 2015.

[14] U. R. Vemulapati, T. Wikström, and M. Lüscher, "An rc-igct for application at up to 5.3kv," in *ICPE 2019 - ECCE Asia*, 2019.

[15] T. Wikstrom, M. Arnold, T. Stiasny, C. Waltisberg, H. Ravener, and M. Rahimo, "The 150 mm RC-IGCT: A device for the highest power requirements," in *2014 IEEE 26th International Symposium on Power Semiconductor Devices & IC's (ISPSD)*, IEEE, jun 2014.

[16] M. Rahimo, "Future trends in high power mos controlled power semiconductors," 2012.

[17] Y. Tang, *Modular Multilevel Converter: Submodule Dimensioning, Testing Method, and Topology Innovation*. PhD thesis, University of Warwick, 2015.

[18] F. Filsecker, R. Alvarez, and S. Bernet, "Comparison of 4.5-kV press-pack IGBTs and IGCTs for medium-voltage converters," *IEEE Transactions on Industrial Electronics*, vol. 60, pp. 440–449, Feb 2013.

[19] Toshiba, "Trends in and future outlook for semiconductor devices with enhanced energy efficiency," tech. rep., Toshiba, 2018.

[20] ABB, "Applying IGCTs," tech. rep., ABB, 2016.

[21] Z. Chen, Z. Yu, X. Liu, J. Liu, and R. Zeng, "Stray impedance measurement and improvement of high-power IGCT gate driver units," *IEEE Transactions on Power Electronics*, vol. 34, no. 7, pp. 6639–6647, 2019.

[22] I. Omura, T. Domon, E. Miyake, Y. Sakiyama, T. Ogura, M. Hiyoshi, N. Yamano, and H. Ohashi, "Electrical and mechanical package design for 4.5kV ultra high power IEGT with 6kA turn-off capability," in *ISPSD '03. 2003 IEEE 15th International Symposium on Power Semiconductor Devices and ICs, 2003. Proceedings.*, pp. 114–117, April 2003.

[23] ABB, "Failure rates of igbt modules due to cosmic rays," tech. rep., ABB, 2017.

[24] M. Perez, J. Rodriguez, J. Pontt, and S. Kouro, "Power distribution in hybrid multi-cell converter with nearest level modulation," in *2007 IEEE International Symposium on Industrial Electronics*, pp. 736–741, June 2007.

[25] Q. Tu, Z. Xu, and L. Xu, "Reduced switching-frequency modulation and circulating current suppression for modular multilevel converters," *IEEE Transactions on Power Delivery*, vol. 26, pp. 2009–2017, jul 2011.